Dalton Transactions

PAPER

View Article Online
View Journal | View Issue

Cite this: *Dalton Trans.*, 2014, **43**, 1599

Synthesis and structural characterisation of Pd(II) and Pt(II) complexes with a flexible, ferrocene-based P,S-donor amidophosphine ligand†

Jiří Tauchman, Ivana Císařová and Petr Štěpnička*

Received 3rd October 2013,
Accepted 29th October 2013

DOI: 10.1039/c3dt52760c

www.rsc.org/dalton

1′-Diphenylphosphino-1-{[(2-(methylthio)ethyl)amino]carbonyl}ferrocene (**1**), accessible *via* amidation of 1′-(diphenylphosphino)ferrocene-1-carboxylic acid (Hdpf) with 2-(methylthio)ethylamine, reacts with [$PdCl_2$(cod)] (cod = cycloocta-1,5-diene) at a 1 : 1 metal-to-ligand ratio to give *trans*-[$PdCl_2$(**1**-κ^2P,S)] (*trans*-**2**) as the sole product. A similar reaction with [$PtCl_2$(cod)] affords a mixture of *cis*- and *trans*-[$PtCl_2$(**1**-κ^2P,S)] (*cis*- and *trans*-**3**), which can be separated by fractional crystallisation. Complexation reactions performed with 2 equiv. of the ligand are less selective, yielding mixtures of the expected bis-phosphine complexes (*i.e.*, *trans*-[$PdCl_2$(**1**-κP)$_2$], or a mixture of *cis*- and *trans*-[$PtCl_2$(**1**-κP)$_2$]) with the respective monophosphine complexes. The structures of **1**, *trans*-**2**, *cis*-**3** and *trans*-**3** determined by X-ray diffraction demonstrate the ability of the title ligand to act as a flexible *cis*- or *trans*-P,S-chelate donor (the ligand bite angles are 174.03(2)/173.05(2)° for *trans*-**2**/**3** and 92.86(2)° for *cis*-**3**).

Introduction

Ligands capable of acting as *trans*-chelate donors are attractive research targets. They not only represent structurally interesting molecules but are also useful tools for the elucidation of structural effects, reaction mechanisms, *etc.*[1] The most often studied *trans*-chelating ligands still remain diphosphines, whose donor moieties are brought into appropriate positions with the aid of a rigid organic backbone.[1,2] Symmetrical ligands featuring other donor atoms (*e.g.*, N,N-donors[3] and bis-carbenes[4]) and, particularly, their donor-asymmetric counterparts are much less common.

For instance, the rare *trans*-chelating P,N-donors are represented by pyridyl-phosphines $Ph_2PC_6H_4CH_2O(CH_2)_n$-(C_5H_4N-2)[5] (n = 1–3) and by (diphenylphosphino)ferrocene derivatives bearing N-heterocyclic substituents in position 1′ of the ferrocene unit.[6] As far as we are aware, however, no similar P,S-bidentate donors have been described in the literature.[7]

Recently, we found that carboxamides **I**–**IV**[8–10] (Scheme 1), prepared from 1′-(diphenylphosphino)ferrocene-1-carboxylic acid (Hdpf)[11] and simple amines equipped with a donor substituent at the terminal position readily form *trans*-chelate complexes with palladium(II) ions. This prompted us to design an analogous, P,S-donor ligand.[12] In this contribution, we describe the preparation and structural characterisation of 1′-diphenylphosphino-1-{[(2-(methylthio)ethyl)amino]carbonyl}-ferrocene (**1**), a congener of the recently described phosphino-carboxamide[13] donors **III** and **IV**,[10] and Pd(II) and Pt(II) complexes obtained thereof.

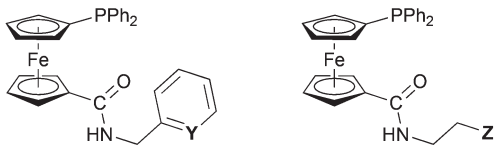

I Y = N
II Y = C–PPh_2
III Z = NMe_2
IV Z = PPh_2

Scheme 1

Results and discussion

Synthesis and characterisation of ligand 1

Phosphino-amide **1** was obtained upon reacting 1′-(diphenylphosphino)ferrocene-1-carboxylic acid (Hdpf) with 2-(methylthio)ethylamine in the presence of a slight excess of 1-hydroxybenzotriazole and 1-ethyl-3-[3-(dimethylamino)-propyl]-carbodiimide as the coupling agents[14] (Scheme 2). The

Department of Inorganic Chemistry, Faculty of Science, Charles University in Prague, Hlavova 2030, 128 40 Prague, Czech Republic. E-mail: stepnic@natur.cuni.cz; Fax: +420 221 951 253

† Electronic supplementary information (ESI) available: Crystal packing diagram for **1**, a view of the molecular structure of *trans*-**2**·$\frac{1}{2}H_2O$, description of the crystal packing of the Pd(II) and Pt(II) complexes, and a summary of the crystallographic data. CCDC 962382–962386. For ESI and crystallographic data in CIF or other electronic format see DOI: 10.1039/c3dt52760c

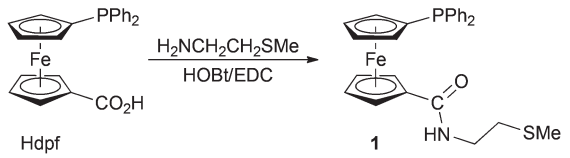

Scheme 2 Preparation of amidophosphine **1** (HOBt = 1-hydroxybenzotriazole, EDC = 1-ethyl-3-[3-(dimethylamino)propyl]carbodiimide.

compound was isolated by column chromatography, resulting as an air-stable, rusty orange solid in 84% yield. The chromatography also afforded a small amount of a more polar side-product, which was identified as the corresponding phosphine oxide **1O** (isolated yield: 7%).

NMR spectra of **1** and **1O** show signals of the terminal SMe groups (δ_H/δ_C: 2.16/14.97 for **1**, and 2.06/14.96 for **1O**) and the ethane-1,2-diyl linkers. Signals due to the PPh_2-substituted ferrocene units are observed at the expected positions and with the characteristic J_{PC} values (*cf.* ref. 8–10). The ^{31}P NMR shifts are −16.9 and 31.6 for **1** and **1O**, respectively. The compounds display typical amide bands (namely ν_{NH} and amide I/II bands) in their IR spectra and give rise to pseudomolecular ions in the ESI mass spectra.

The molecular structures of **1** and **1O** determined by single-crystal X-ray diffraction analysis are depicted in Fig. 1 and 2. Selected geometric data are given in Table 1. The ferrocene moieties in the molecules of **1** and **1O** are regular showing tilt angles below *ca.* 5° and, accordingly, similar individual Fe–C distances (2.030(2)–2.059(2) Å for **1**, and 2.024(2)–2.062(2) Å for **1O**). However, their substituents assume different mutual orientations (see τ angles in Table 1). While the conformation of **1** is anticlinal eclipsed, the substituents in **1O** are moved closer to a synclinal eclipsed conformation by the intramolecular N–H···O=P hydrogen bond. In both cases, the amide planes and the planes of their parent cyclopentadienyl ring are twisted (see φ in Table 1) so that the amide nitrogen is directed towards the side of the ferrocene unit. The amide substituents in **1** and **1O** adopt similar orientations pointing toward the other Cp ring and have the substituents at the C24–C25 bond at *ca.* 60° or in *gauche* conformation.

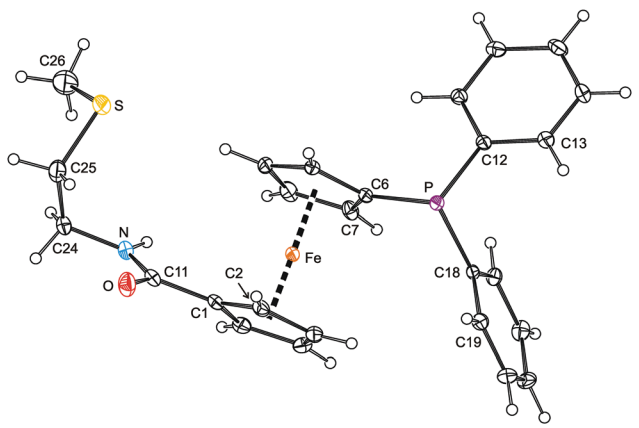

Fig. 1 View of the molecular structure of **1** showing the atom labelling scheme. Displacement ellipsoids are scaled to the 30% probability level.

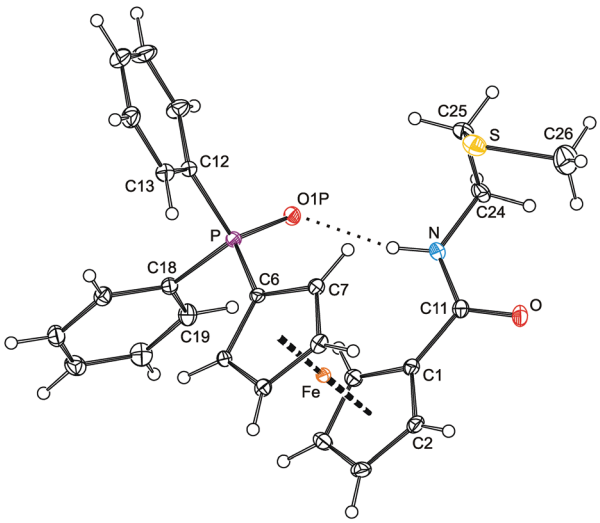

Fig. 2 View of the molecular structure of phosphine oxide **1O** showing the atom labelling scheme. Displacement ellipsoids enclose the 30% probability level. The N–H1N···O1P hydrogen bond is indicated with a dotted line (N···O1P = 2.920(2) Å, angle at H1N = 167°).

Table 1 Selected intramolecular distances and angles for **1** and **1O** (in Å and °)

Parameter[a]	**1**	**1O**[e]
Fe–Cg1	1.6492(9)	1.650(1)
Fe–Cg2	1.6427(9)	1.646(1)
∠Cp1, Cp2	4.5(1)	2.4(1)
τ^b	144.9(1)	71.7(2)
P–C6	1.808(2)	1.786(2)
P–C12/18	1.837(2)/1.834(2)	1.803(2)/1.809(2)
C–P–C[c]	101.16(7)–104.53(7)	104.8(1)–106.1(1)
C11–O	1.228(2)	1.233(3)
C11–N	1.348(3)	1.348(3)
O–C11–N	122.9(2)	123.8(2)
φ^d	30.3(2)	23.7(3)
N–C24–C25–S	61.9(2)	63.2(2)
C25–S–C26	100.9(1)	100.4(1)

[a] The ring planes are defined as follows: Cp1 = C(1–5), Cp2 = C(6–10). Cg1/2 are the respective ring centroids. [b] Torsion angle C1–Cg1–Cg2–C6. [c] The range of C6–P–C(12/18) and C12–P–C18 angles. [d] Dihedral angle subtended by the amide unit (C11, O, N) and the ring Cp1. [e] Additional data: P–O1P = 1.496(2) Å; O1P–P–C(6/12/18) = 112.5(1)–114.5(1)°.

Preparation of Group 10 metal complexes

Divalent Group 10 metal ions were chosen for an evaluation of the coordination properties of compound **1** mainly because they include the borderline Ni(II) as well as the typical soft Pd(II)/Pt(II) metal ions showing different kinetic properties.[15,16] Unfortunately, repeated attempts at obtaining some Ni(II)-**1** complexes failed. The reactions of $[NiCl_2(dme)]$ (dme = 1,2-dimethoxyethane) or $NiCl_2{\cdot}6H_2O$ with 1 equiv. of **1** afforded only rapidly decomposing mixtures, from which no defined product could be isolated. This may reflect a mismatch situation

resulting from a relatively smaller size of the Ni(II) ion and the soft character of the donor atoms present in **1**.

In contrast, the reaction of **1** with [$PdCl_2$(cod)] (cod = cycloocta-1,5-diene; Pd : **1** = 1 : 1) proceeded rapidly and cleanly to provide a single product showing its ^{31}P NMR signal at a lower field (δ_P 23.6, Δ_P = 40.5 ppm) compared with the free ligand. This shift, together with a low-field shift of the SMe resonance (Δ_H = 0.13 ppm) and its splitting with the ^{31}P nucleus ($^4J_{PH}$ = 4.7 Hz), already suggested chelate coordination of ligand **1**. Indeed, this was corroborated by X-ray crystallography showing the product to be the *trans*-chelate complex *trans*-[$PdCl_2$(**1**-κ^2*S*,*P*)] (*trans*-**2** in Scheme 3).

Compound *trans*-**2** shows broad ^{1}H NMR signals for protons at the ferrocene unit and in the ethane-1,2-diyl bridge at room temperature.[17] Nonetheless, this broadening is in line with the formulation as it reflects a limited molecular mobility resulting from spatial constraints imposed by a tight chelate coordination. The amide vibrations of *trans*-**2** are observed shifted *vs.* free **1** (amide I and II by *ca.* +30 and −10 cm^{-1}, respectively) whilst the amide ^{13}C NMR resonance (C═O) remains nearly unaffected. The complex displays a pseudo-molecular ion ([M + Na]$^+$) and fragment ions attributable to [M − Cl − HCl]$^+$ and [Pd(Ph_2Pfc)]$^+$ (fc = ferrocene-1,1′-diyl) in its ESI MS spectrum.

An analogous reaction of **1** with [$PtCl_2$(cod)] (Scheme 3; $CHCl_3$/refluxing for 3 h) afforded a mixture of two compounds showing different ^{31}P NMR shifts and $^1J_{PtP}$ coupling constants. Considering the fact that even the signals of the SMe protons were flanked with ^{195}Pt satellites, the products were formulated as isomeric P,S-chelate complexes *cis*-**3** (δ_P 5.3, $^1J_{PtP}$ = 3695 Hz; *ca.* 35%) and *trans*-**3** (δ_P 6.6, $^1J_{PtP}$ = 3495 Hz; *ca.* 65%),[18] being distinguished through the $^1J_{PtP}$ coupling constants.[19] The isomers differ also in their ^{1}H NMR spectra displaying four degenerate signals and eight anisochronic (diastereotopic) signals for the ferrocene protons in *trans*-**3** and *cis*-**3**, respectively.

Fortunately, the isomeric complexes *trans*-**3** and *cis*-**3** could be separated by fractional crystallisation (isolated yields: *cis*-**3** 51%, *trans*-**3** 26%) and were subjected to X-ray diffraction analysis, which confirmed the assigned structures (see below).

Complexation reactions performed at 1 : 2 metal-to-ligand ratios proved more complicated. The crude reaction mixture obtained after mixing [$PdCl_2$(cod)] with two molar equivalents of **1** (90 min/room temperature) contained three different compounds, which were identified by ^{31}P NMR spectroscopy as *trans*-**2**, **1O** (both minor components) and the expected bis-phosphine complex, *trans*-[$PdCl_2$(**1**-κ*P*)$_2$] (*trans*-**4**). Repeated attempts to isolate this major product (*ca.* 85% in the reaction mixture) by crystallisation failed and the compound could therefore only be characterised by NMR spectroscopy in a solution.

A similar reaction between [$PtCl_2$(cod)] and two equivalents of **1** (at room temperature for 90 min) afforded a mixture of *five* different compounds. ^{31}P NMR monitoring revealed the presence of **1O**, *cis*- and *trans*-**3** (all minor components) and two isomeric bis-phosphine complexes, *cis*- and *trans*-[$PtCl_2$(**1**-κ*P*)$_2$] (**5**). Likewise *cis*- and *trans*-**3**, the isomers of complex **5**, can be clearly differentiated by means of ^{31}P NMR spectroscopy[19a,b] (*cis*-**5**: δ_P 10.2, $^1J_{PtP}$ = 3790 Hz; *trans*-**5**: δ_P 10.9, $^1J_{PtP}$ = 2615 Hz). In accordance with the geometry of the leaving ligand and kinetic inertness of Pt(II) species, the bis-phosphine complexes were formed in *cis* : *trans* ratio of *ca.* 2 : 1 which, however, changed in favour of the thermodynamically preferred *trans*-isomer after refluxing for 18 h (*cis* : *trans* = 1 : 2). When the Pt-precursor was replaced with K[$PtCl_3$(η^2-C_2H_4)], whose alkene ligand destabilises the chloride in mutual *trans* position owing to its large *trans*-influence,[20] the product ratio determined initially (room temperature/90 min) was inverted (*cis* : *trans* = 1 : 2) and did not change upon refluxing for 18 h. Even in this case, however, minor amounts of **1O**, *cis*- and *trans*-**3** were detected in the reaction mixture.

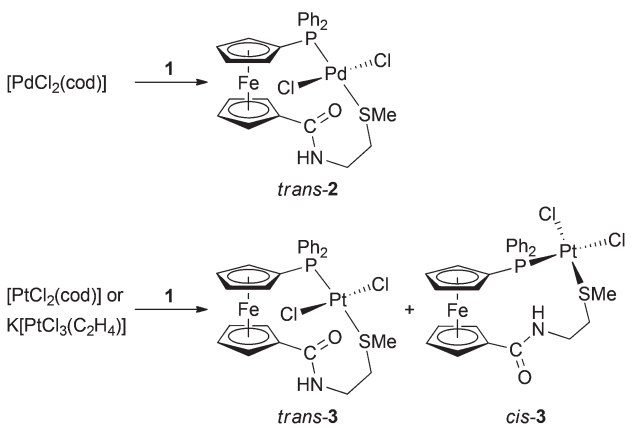

Scheme 3 Preparation of complexes **2** and **3** (cod = cycloocta-1,5-diene).

The molecular structures of the Pd(II) and Pt(II) complexes

As indicated above, the structures of *trans*-**2**, *trans*-**3** and *cis*-**3** were determined by X-ray diffraction analysis. Only the latter compound was isolated in an unsolvated form while the *trans*-complexes accommodated molecules of adventitious water (*trans*-**2**) or the crystallisation solvent (*trans*-**3**) in their structures (for a discussion of the crystal packing, see ESI†). The molecular structures of *cis*- and *trans*-**3** are presented in Fig. 3. A structural diagram for *trans*-**2** is available as ESI (Fig. S2†). Relevant geometric data are summarised in Table 2.

The complexes adopt the expected square-planar geometry so that the central atoms and their four ligating atoms are coplanar within less than 0.001 Å in *trans*-**2**, *ca.* 0.03 Å in *trans*-**3** and *ca.* 0.16 Å in *cis*-**3**. Rather surprisingly, the largest deviation from a coplanar arrangement detected for the latter complex is associated with the smallest departure of the individual inter-ligand angles from the ideal 90° (*ca.* 88–93°). Inter-ligand angles in the *trans*-complexes range *ca.* 83–94°, with the extreme values pertaining to the S–M–Cl1/2 angles.

The M-donor distances are found within the usual ranges,[21] yet they nicely demonstrate the different *trans*-influence of the ligands (PR_3 > SR_2 ≫ Cl^-)[20] and the fact that two soft donor

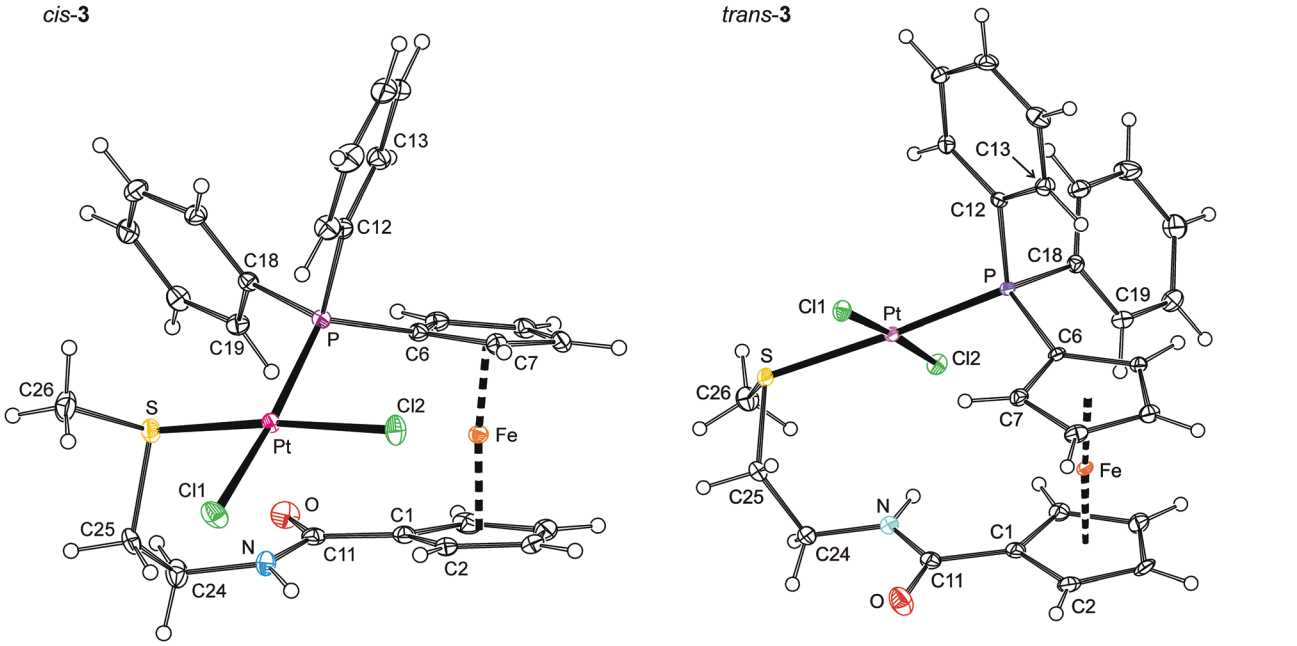

Fig. 3 View of the complex molecules in the structures of *cis*-**3** (left) and *trans*-**3**·1/2$CH_3CO_2C_2H_5$ (right). Displacement ellipsoids enclose the 30% probability level.

Table 2 Selected distances and angles for compounds *trans*-**2**·1/2H_2O, *trans*-**3**·1/2CH_3CO_2Et, and *cis*-**3** (in Å and °)

Parameter[a]	*trans*-**2**·1/2H_2O	*trans*-**3**·1/2CH_3CO_2Et	*cis*-**3**
M	Pd	Pt	Pt
M–P	2.2628(4)	2.2601(6)	2.2436(5)
M–S	2.3992(4)	2.3677(6)	2.2809(5)
M–Cl1	2.2931(5)	2.3051(5)	2.3564(6)
M–Cl2	2.2894(5)	2.3043(5)	2.3153(5)
P–M–S	174.03(2)	173.05(2)	92.86(2)
P–M–Cl1	90.11(2)	90.08(2)	—
S–M–Cl1	83.95(2)	83.00(2)	89.84(2)
P–M–Cl2	91.66(2)	93.05(2)	90.37(2)
S–M–Cl2	94.28(2)	93.88(2)	—
Cl1–M–Cl2	—	—	87.87(2)
Fe–Cg1	1.6547(8)	1.657(1)	1.651(1)
Fe–Cg2	1.6517(8)	1.651(1)	1.647(1)
∠Cp1, Cp2	3.5(1)	4.4(1)	5.5(1)
τ^b	−66.9(1)	−67.7(2)	33.4(2)
C11–O	1.233(2)	1.219(3)	1.234(3)
C11–N	1.347(2)	1.360(4)	1.349(3)
O–C11–N	122.4(2)	122.8(2)	123.1(2)
φ^c	7.6(2)	7.7(3)	11.3(2)
N–C24–C25–S	68.6(2)	64.7(3)	60.7(2)
C25–S–C26	102.10(8)	102.2(1)	99.5(1)

[a] The ring planes are defined as follows: Cp1 = C(1–5), Cp2 = C(6–10). Cg1 and Cg2 stand for the respective ring centroids. [b] Torsion angle C1–Cg1–Cg2–C6. [c] Dihedral angle subtended by the amide plane (C11, O, N) and its bonding ring Cp1.

moieties (with a high *trans*-influence) bonding to a soft metal ion in mutually *trans* positions destabilise each other.[22,23] Thus, the Pt–P and, particularly, the Pt–S bonds are longer in *trans*-**3** than in *cis*-**3**,[24] while for *cis*-**3**, the Pt–Cl distance *trans* to P is significantly longer than that *trans* to S. It is also noteworthy that because of practically identical radii of Pd(II) and Pt(II),[25] and identical coordination environments, the overall structures of *trans*-**2** and *trans*-**3** are very similar. The M-donor (M = Pd, Pt) bond distances and inter-ligand angles in these complexes differ by no more than *ca.* 0.03 Å and 1°, respectively.

In order to comply with the demands of the coordinated metal ions, the ligand molecule undergoes a pronounced conformational reorganisation. The major changes are seen at the ferrocene unit, whose substituents are rotated to positions more proximal than in the structure of uncoordinated **1**. In *trans*-**2** and **3**, the ferrocene units are synclinal eclipsed, and in *cis*-**3** they assume an even closer position near to staggered synclinal. The amide units are also rotated from positions observed in free **1** (by *ca.* 40°) so that the N atoms are forced away from the ferrocene unit, slightly more in *cis*-**3** than in the *trans*-complexes. On the other hand, the tilt angles remain rather low, the largest tilting being 5.5(1)° for *cis*-**3**. The orientation of the substituents at the C24–C25 are virtually the same as that in the free ligand, but the bond is differently orientated towards the plane of the amide-substituted cyclopentadienyl ring.[26] The C–P–C angles and C25–S–C26 angles change only marginally.

Electrochemistry

The electrochemical behaviour of ligand **1**, phosphine oxide **1O** and Pd(II) complex *trans*-**2** was studied by cyclic and differential pulse voltammetry at a glassy carbon disc electrode in 1,2-dichloroethane containing 0.1 M $Bu_4N[PF_6]$ as the supporting electrolyte.

Compound **1** showed three consecutive oxidations within the accessible potential range (Fig. 4). The first oxidation

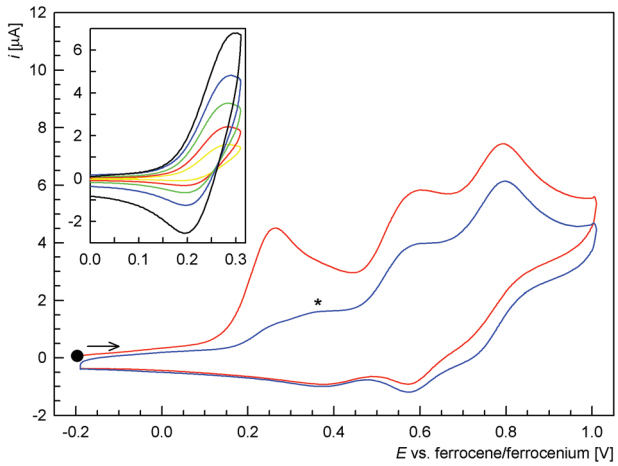

Fig. 4 Cyclic voltammogram of **1** recorded in 1,2-dichloroethane on a glassy carbon electrode (first scan in red, second scan in blue). The signal marked with an asterisk is presumably due to **1O**. The inset shows partial cyclic voltammograms recorded at different scan rates (yellow 0.02 V s^{-1}, red 0.05 V s^{-1}, green 0.10 V s^{-1}, blue 0.20 V s^{-1}, and black 0.50 V s^{-1}).

observed at E_{pa} = 0.28 V *vs.* ferrocene/ferrocenium[27] was quasi-reversible. At relatively lower scan rates or when the switching potential was set to more positive values, it appeared electrochemically irreversible. However, when scanned separately and with higher scan rates, a reductive counter-wave could be detected (see inset in Fig. 4).[28]

The subsequent oxidations seen at E_{pa} = 0.60 and 0.80 V were also irreversible and probably composite in nature. Their complex nature was manifested in the difference pulse voltammograms (Fig. 5). It is also noteworthy that another wave, partly replacing the first oxidation wave, emerged upon repeated scanning (see Fig. 4, signal marked with an asterisk). Based on a comparison of the redox potentials and in view of our previous work,[11a] this wave could be tentatively assigned to the oxidation of **1O** resulting from primary, ferrocene-based

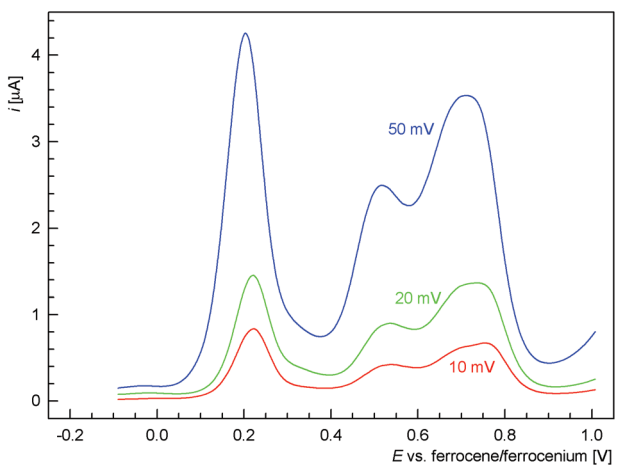

Fig. 5 Differential pulse voltammograms of **1** recorded in 1,2-dichloroethane on a glassy carbon electrode and with different modulation amplitudes (given in the figure).

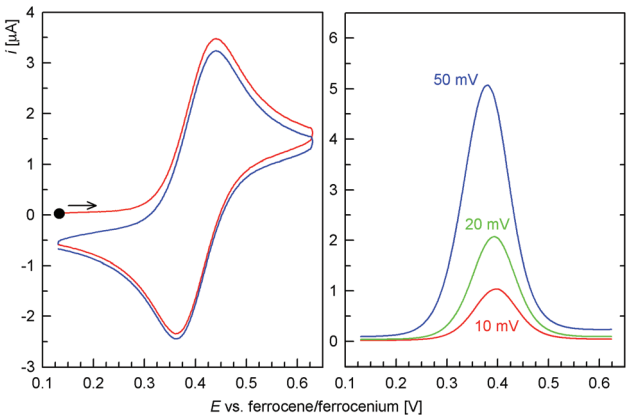

Fig. 6 Representative cyclic (left; scan rate 0.1 V s^{-1}) and differential pulse (right) voltammograms of **1O** recorded in 1,2-dichloroethane on a glassy carbon electrode. The voltammograms are presented with the same scale; modulation amplitude for the differential pulse voltammograms is given in the figure.

oxidation and the associated follow-up chemical reactions of the unstable ferrocenium intermediate.[29]

Unlike **1**, the redox behaviour of the corresponding phosphine oxide **1O** was simple (Fig. 6). The compound, lacking the lone pair of phosphorus as a reactive site, underwent a single, one-electron reversible oxidation at $E^{o\prime}$ = 0.40 V. The separation of the peaks in cyclic voltammograms was *ca.* 80 mV at a scan rate of 0.1 V s^{-1}.[30] The anodic and cathodic peak currents increased linearly with the square root of the scan rate ($i_p \propto \nu^{1/2}$) and their ratio remained close to unity over the range 0.02–1.0 V s^{-1}. This oxidation, attributed to the ferrocene/ferrocenium couple, appeared shifted to more positive potentials than the ferrocene reference, in accordance with the electron-withdrawing nature of the substituents attached to the ferrocene unit (*cf.* the Hammett's σ_p constants:[31] CONHMe 0.35, PPh_2 0.19, $P(O)Ph_2$ 0.53) that render the oxidation more difficult.

Similarly to **1O**, complex *trans*-**2** (Fig. 7) displayed a one-electron, reversible oxidation at $E^{o\prime}$ = 0.46 V.[32] This wave was

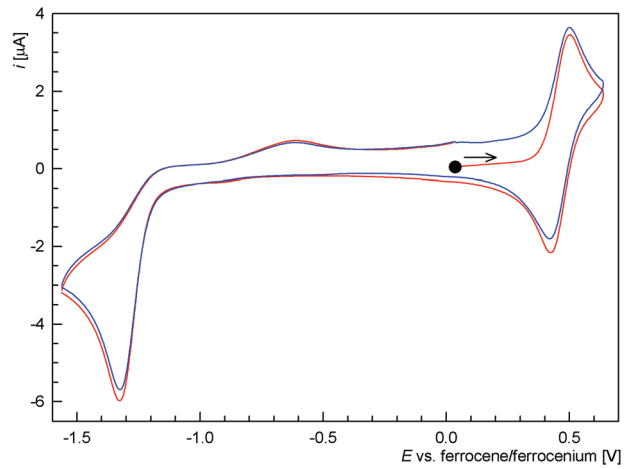

Fig. 7 Cyclic voltammogram of *trans*-**2** recorded in 1,2-dichloroethane on a glassy carbon electrode (first scan in red, second scan in blue).

shifted with respect to the free ligand, most likely owing to an electron density transfer from the ligand (ferrocene unit) upon coordination. An additional irreversible, multi-electron reduction was observed at $E_{pc} = -1.34$ V[27] *vs.* ferrocene/ferrocenium. Together with an associated, small oxidation wave at E_{pc} *ca.* −0.61 V, this probably reflects an irreversible reductive removal of one Pd-bound chloride as described previously for $[PdCl_2(PPh_3)_2]$.[33]

Conclusions

Functional ferrocene-based phosphino-amide **1** is readily accommodated as a P,S-donor in both the *cis*- and *trans*-MCl_2 square-planar fragments of the heavier Group 10 metal ions. The latter coordination mode appears particularly remarkable because the ligand is structurally flexible and donor-asymmetric, unlike the majority of *trans*-spanning donors known to date. Furthermore, the results presented earlier for the structurally related ligands **I–IV** (see Introduction) and herein for compound **1**, demonstrate that the formation of *trans*-chelate complex donors does not necessarily require the prospective *trans*-spanning donor to comprise a rigid organic backbone if this is replaced with appropriately selected structural fragments. Further work focusing on other metal ions and a comparison of the structurally related donors **1**, **III** and **IV** is currently underway.

Experimental

Materials and methods

All manipulations were performed under an argon atmosphere and with the exclusion of direct daylight. Chloroform and dichloromethane were dried by standing over K_2CO_3 and distilled under argon. Methanol was distilled from MeONa. Solvents (from Lachner) for work-up and crystallisations were used without any additional purification. Hdpf,[11a] $[MCl_2(cod)]$ (M = Pd, Pt),[34] and $K[PtCl_3(C_2H_4)]$[35] were prepared according to the literature procedures. All other chemicals were obtained from Sigma-Aldrich.

NMR spectra were recorded at 25 °C using a Varian UNITY Inova 400 MHz spectrometer operating at 399.95 MHz for ^{1}H, at 100.58 MHz for ^{13}C, and at 161.90 for ^{31}P, if not specified otherwise. Chemical shifts (δ/ppm) are given relative to internal tetramethylsilane (^{1}H and ^{13}C) and to external 85% H_3PO_4 (^{31}P). Infrared spectra were recorded with an FT IR Nicolet Magna 760 spectrometer in the range 400–4000 cm^{-1}. Electrospray ionisation (ESI) mass spectra were obtained with an Esquire 3000 (Bruker; low resolution) or an LTQ Orbitrap XL instrument (Thermo Fisher Scientific; high resolution).

Syntheses

1′-Diphenylphosphino-1-{[(2-(methylthio)ethyl)amino]carbonyl}ferrocene (1). A suspension of Hdpf (414 mg, 1.00 mmol) and 1-hydroxybenzotriazole monohydrate (184 mg, 1.20 mmol) in dry dichloromethane (15 mL) was cooled in an ice bath and treated with 1-[3-(dimethylamino)propyl]-3-ethylcarbodiimide (0.21 mL, 1.20 mmol). The resulting mixture was stirred at 0 °C for 15 min, whereupon the solids dissolved to give a clear orange-red solution. Then, a solution of $H_2NCH_2CH_2SMe$ (0.12 mL, 1.20 mmol) in dichloromethane (5 mL) was introduced, and the cooling bath was removed. The reaction mixture was stirred overnight at room temperature and then washed successively with saturated aqueous $NaHCO_3$ (2 × 50 mL) and brine (50 mL). The organic phase was separated, dried over $MgSO_4$ and evaporated under vacuum, leaving an orange oily residue which was purified by column chromatography over silica gel using dichloromethane–methanol 50 : 1 (v/v) as the eluent. Two orange-yellow bands were collected and evaporated to afford analytically pure phosphine **1** as an orange solid (409 mg, 84%; the first band) and the respective phosphine-oxide **1O** (yellow-brown solid, 33 mg, 7%; second band).

Analytical data for 1. ^{1}H NMR ($CDCl_3$): δ 2.16 (s, 3 H, SMe), 2.73 (t, $^3J_{HH}$ = 6.4 Hz, 2 H, SCH_2), 3.57 (q, $^3J_{HH}$ = 6.3 Hz, 2 H, $HNCH_2$), 4.15 (virtual q, J = 1.9 Hz, 2 H, fc), 4.26 (virtual t, J = 1.9 Hz, 2 H, fc), 4.48 (virtual t, J = 1.8 Hz, 2 H, fc), 4.61 (virtual t, J = 2.0 Hz, 2 H, fc), 6.20 (t, $^3J_{HH}$ = 5.4 Hz, 1 H, NH), 7.35–7.44 (m, 10 H, PPh_2). ^{13}C{^{1}H} NMR ($CDCl_3$): δ 14.97 (SMe), 34.00 (SCH_2), 37.70 ($HNCH_2$), 69.46 (*C*H fc), 71.56 (*C*H fc), 72.86 (d, J_{PC} = 3 Hz, *C*H fc), 74.38 (d, J_{PC} = 13 Hz, *C*H fc), 76.77 (*C*-CONH fc), 128.29 (d, $^3J_{PC}$ = 7 Hz, *C*H PPh_2), 128.77 (*C*H PPh_2), 133.47 (d, $^2J_{PC}$ = 20 Hz, *C*H PPh_2), 138.23 (d, $^1J_{PC}$ = 8 Hz, C_{ipso} PPh_2), 169.92 (CONH). The signal due to C–P of fc was not found probably due to overlaps. ^{31}P{^{1}H} NMR ($CDCl_3$): δ −16.9 (s). IR (Nujol): ν_{NH} 3336 m, amide I 1627 vs, amide II 1541 vs, 1438 s, 1295 s, 1235 w, 1181 m, 1160 m, 1092 w, 1062 w, 1047 w, 1027 m, 999 w, 947 w, 831 s, 822 m, 774 w, 740 s, 698 s, 636 w, 541 w, 499 s, 452 m, 420 w cm^{-1}. MS (ESI+): *m*/*z* 526 ($[M + K]^+$), 510 ($[M + Na]^+$), 488 ($[M + H]^+$). Anal. Calcd for $C_{26}H_{26}NOPSFe$ (487.4): C 64.07, H 5.38, N 2.87. Found: C 63.79, H 5.28, N 2.79.

Analytical data for 1O. ^{1}H NMR ($CDCl_3$): δ 2.06 (s, 3 H, SMe), 2.76 (t, $^3J_{HH}$ = 7.1 Hz, 2 H, SCH_2), 3.59 (q, $^3J_{HH}$ = 6.6 Hz, 2 H, $HNCH_2$), 4.13 (virtual t, J = 2.0 Hz, 2 H, fc), 4.26 (virtual q, J = 1.9 Hz, 2 H, fc), 4.57 (virtual q, J = 1.8 Hz, 2 H, fc), 5.03 (virtual t, J = 2.0 Hz, 2 H, fc), 7.44–7.58 (m, 6 H, PPh_2), 7.65–7.73 (m, 4 H, PPh_2), 9.08 (t, $^3J_{HH}$ = 5.3 Hz, 1 H, NH). ^{13}C{^{1}H} NMR ($CDCl_3$): δ 14.96 (SMe), 33.32 (SCH_2), 38.50 ($HNCH_2$), 70.39 (*C*H fc), 70.75 (*C*H fc), 72.55 (d, J_{PC} = 10 Hz, *C*H fc), 73.56 (d, $^1J_{PC}$ = 114 Hz, C-P fc), 75.23 (d, J_{PC} = 13 Hz, *C*H fc), 79.22 (*C*-CONH fc), 128.41 (d, $^3J_{PC}$ = 12 Hz, *C*H PPh_2), 131.43 (d, $^2J_{PC}$ = 10 Hz, *C*H PPh_2), 131.93 (d, $^4J_{PC}$ = 2 Hz, *C*H PPh_2), 132.91 (d, $^1J_{PC}$ = 107 Hz, C_{ipso} PPh_2), 170.00 (CONH). ^{31}P{^{1}H} NMR ($CDCl_3$): δ 31.6 (s). IR (Nujol): ν_{NH} 3236 m, amide I 1649 vs, amide II 1550 s, 1437 s, 1292 s, 1202 m, 1189 m, 1161 vs, 1121 m, 1099 w, 1070 w, 1055 w, 1036 m, 997 w, 963 w, 904 w, 845 m, 818 m, 751 m, 702 s, 617 w, 570 vs, 536 s, 504 s, 475 m, 446 w cm^{-1}. MS (ESI+): *m*/*z* 542 ($[M + K]^+$), 526 ($[M + Na]^+$), 504 ($[M + H]^+$). HR MS (ESI+) calc. for $C_{18}H_{16}O_2N_2FeNa$ $[M + Na]^+$ 526.0664, found 526.0662. Anal. Calcd for $C_{26}H_{26}NO_2PSFe$ (503.4): C 62.04, H 5.21, N 2.78. Found: C 62.08, H 5.40, N 2.76.

***trans*-[$PdCl_2$(1-κ^2*S*,*P*)] (*trans*-2).** A solution of **1** (49 mg, 0.10 mmol) in chloroform (2 mL) was added to solid

[$PdCl_2$(cod)] (29 mg, 0.10 mmol). The dark red solution formed was stirred for 1 h and filtered through a PTFE syringe filter (pore size 0.45 μm) into pentane (70 mL). After standing at −18 °C overnight, the precipitated product was filtered off, washed with pentane (3 × 5 mL) and dried under vacuum to afford analytically pure complex *trans*-**2** as an orange amorphous solid. Yield: 57 mg, 86%.

^{1}H NMR ($CDCl_3$, 50 °C): δ 2.29 (d, $^4J_{PH}$ = 4.7 Hz, 3 H, SMe), 3.13 (q, J = 5.3 Hz, 2 H, SCH_2), 3.79 (br s, 2 H, HNCH_2), 4.52 (virtual t, J = 2.0 Hz, 2 H, fc), 4.72 (s, 2 H, fc), 4.80 (br s, 2 H, fc), 5.36 (virtual t, J = 1.7 Hz, 2 H, fc), 7.32–7.47 (m, 6 H, PPh_2), 7.51 (t, $^3J_{HH}$ = 5.2 Hz, 1 H, NH), 7.61–7.71 (m, 4 H, PPh_2). $^{31}P\{^1H\}$ NMR ($CDCl_3$): δ 23.6 (s). IR (Nujol): ν_{NH} 3366 m, amide I 1659 vs, amide II 1529 vs, 1436 vs, 1306 m, 1284 m, 1170 m, 1098 m, 1056 w, 1033 m, 1000 w, 966 w, 847 w, 821 w, 769 w, 746 m, 708 w, 692 s, 623 w, 548 w, 521 s, 505 m, 475 s, 440 w, 417 w cm^{-1}. MS (ESI+): m/z 688 ([M + Na]$^+$), 526 ([M − HCl − Cl]$^+$), 475 (presumably [Ph_2PfcPd]$^+$). Anal. Calcd for $C_{26}H_{26}NOPSCl_2FePd{\cdot}0.25CHCl_3$ (694.5): C 45.39, H 3.81, N 2.02. Found: C 45.44, H 3.82, N 1.84.

Reaction of [$PtCl_2$(cod)] with one molar equivalent of 1. A solution of **1** (30 mg, 0.06 mmol) in chloroform (3 mL) was added to solid [$PtCl_2$(cod)] (23 mg, 0.06 mmol) and the resulting red solution was refluxed for 3 h. After cooling to room temperature, the mixture was evaporated under vacuum and the residue was analysed by ^{1}H and $^{31}P\{^1H\}$ NMR spectroscopy. The spectra showed two sets of signals attributable to Pt-**1** species. Separation of the products was achieved by fractional crystallisation as follows.

A chloroform solution (*ca*. 1 mL) of the crude product was layered with hexane. Subsequent crystallisation at room temperature for several days afforded orange crystals of *cis*-**3**, which were filtered off, washed with hexane (3 mL) and pentane (3 × 3 mL) and dried under vacuum. Yield after two crystallisations: 25 mg (51%), orange crystals. The mother liquor was evaporated and the residue was dissolved in ethyl acetate. The solution was layered with pentane and allowed to crystallise by liquid-phase diffusion for several days. The yellow-orange crystals of *trans*-**3** that formed were filtered off, washed with pentane and dried under vacuum. Yield of *trans*-**3**: 12 mg, 26%.

Characterisation data for *cis*-[$PtCl_2$(1-κ^2*S*,*P*)] (*cis*-3). ^{1}H NMR ($CDCl_3$): δ 2.52 (s with broad ^{195}Pt satellites, $^3J_{PtH}$ = 48.3 Hz, 3 H, SMe), 2.72–2.83 (m, 1 H, SCH_2), 3.51–3.60 (m, 1 H, SCH_2), 4.10–4.23 (m, 2 H, HNCH_2), 4.40 (dt, J = 2.6, 1.2 Hz, 1 H, fc), 4.44 (dq, J = 4.0, 1.6 Hz, 1 H, fc), 4.48 (dq, J = 2.7, 1.4 Hz, 1 H, fc), 4.55 (dq, J = 3.8, 1.3 Hz, 1 H, fc), 4.66 (dt, J = 2.6, 1.4 Hz, 1 H, fc), 5.14 (dt, J = 2.7, 1.4 Hz, 1 H, fc), 5.47 (dq, J = 2.8, 1.4 Hz, 1 H, fc), 5.58 (dt, J = 2.8, 1.4 Hz, 1 H, fc), 7.06–7.23 (m, 2 H of PPh_2 and 1 H of NH), 7.35–7.52 (m, 6 H, PPh_2), 7.58–7.66 (m, 2 H, PPh_2). $^{31}P\{^1H\}$ NMR ($CDCl_3$): δ 5.3 (s with ^{195}Pt satellites, $^1J_{PtP}$ = 3695 Hz). IR (Nujol): ν_{NH} 3386 m, amide I 1632 vs, 1586 w, amide II 1525 vs, 1436 s, 1419 w, 1354 w, 1312 w, 1283 m, 1240 w, 1171 m, 1165 m, 1101 m, 1060 w, 1046 m, 1030 m, 999 w, 975 w, 961 w, 828 m, 806 w, 763 s, 743 s, 713 m, 698 s, 665 w, 548 m, 527 m, 496 w, 483 s, 440 m, 416 w cm^{-1}. MS (ESI+): m/z 776 ([M + Na]$^+$), 681 ([M − HCl − Cl]$^+$). Anal. Calcd for $C_{26}H_{26}NOPSCl_2FePt{\cdot}0.5CHCl_3$ (813.0): C 39.15, H 3.29, N 1.72. Found: C 39.18, H 3.26, N 1.56.

Characterisation data for *trans*-[$PtCl_2$(1-κ^2*S*,*P*)] (*trans*-3). ^{1}H NMR ($CDCl_3$): δ 2.41 (d, J = 4.2 Hz with br ^{195}Pt satellites, $^3J_{PtH}$ = 23.0 Hz, 3 H, SMe), 3.25 (br s, 2 H, SCH_2), 3.83 (br s, 2 H, HNCH_2), 4.57 (virtual t, J = 1.9 Hz, 2 H, fc), 4.75 (s, 2 H, fc), 4.82 (br s, 2 H, fc), 5.30 (s, 2 H, fc), 7.35–7.47 (m, 6 H, PPh_2), 7.59 (br t, $^3J_{HH}$ = 5.7 Hz, 1 H, NH), 7.64–7.76 (m, 4 H, PPh_2). $^{31}P\{^1H\}$ NMR ($CDCl_3$): δ 6.6 (s with ^{195}Pt satellites, $^1J_{PtP}$ = 3495 Hz). IR (Nujol): ν_{NH} 3375 m, amide I 1652 vs, amide II 1533 vs, 1436 s, 1411 w, 1303 s, 1280 m, 1198 w, 1180 s, 1172 s, 1101 s, 1051 w, 1036 s, 1011 w, 960 w, 881 w, 848 m, 834 w, 820 m, 756 s, 746 s, 708 w, 696 s, 626 w, 609 w, 556 m, 527 s, 496 s, 478 s, 439 m, 417 w cm^{-1}. MS (ESI+): m/z 776 ([M + Na]$^+$), 681 ([M − HCl − Cl]$^+$). Anal. Calcd for $C_{26}H_{26}NOPSCl_2FePd$ (753.3): C 41.45, H 3.48, N 1.86. Found: C 41.18, H 3.26, N 1.60.

Attempted reaction of 1 with [$NiCl_2$(dme)] or $NiCl_6{\cdot}6H_2O$. A solution of **1** (15 mg, 0.03 mmol) in absolute ethanol (1 mL) was added to a suspension of [$NiCl_2$(dme)] (7 mg, 0.03 mmol, dme = 1,2-dimethoxyethane) or $NiCl_6{\cdot}6H_2O$ (7 mg, 0.03 mmol) in the same solvent (1 mL). The mixture was stirred at room temperature for 1 h. Subsequent evaporation of the mixture caused extensive decomposition.

Reaction of [$PdCl_2$(cod)] with two equivalents of 1. A solution of ligand **1** (20 mg, 0.04 mmol) in chloroform (2 mL) was added to solid [$PdCl_2$(cod)] (6 mg, 0.02 mmol). The resulting red mixture was stirred at room temperature for 1 h and evaporated under vacuum. ^{1}H NMR and $^{31}P\{^1H\}$ NMR spectra revealed three sets of signals due to **1** and *trans*-**2** (both in traces) and *trans*-[$PdCl_2$(1-κ*P*)$_2$] (*trans*-**4**; major).

Characterisation data for *trans*-4. ^{1}H NMR ($CDCl_3$): δ 2.09 (s, 3 H, SMe), 2.60 (t, $^3J_{HH}$ = 6.7 Hz, 2 H, SCH_2), 3.44 (q, $^3J_{HH}$ = 6.4 Hz, 2 H, HNCH_2), 4.49 (virtual t, J = 1.8 Hz, 2 H, fc), 4.58 (virtual t, J = 1.7 Hz, 2 H, fc), 4.64 (virtual t, J = 1.9 Hz, 2 H, fc), 4.88 (virtual t, J = 1.9 Hz, 2 H, fc), 6.39 (t, $^3J_{HH}$ = 5.8 Hz, 1 H, NH), 7.30–7.49 (m, 6 H, PPh_2), 7.60–7.70 (m, 4 H, PPh_2). $^{31}P\{^1H\}$ NMR ($CDCl_3$): δ 15.8 (s).

Reaction of [$PtCl_2$(cod)] with two equivalents of 1. A solution of **1** (20 mg, 0.04 mmol) in chloroform (2 mL) was added to solid [$PtCl_2$(cod)] (8 mg, 0.02 mmol). The resulting orange-red mixture was stirred at room temperature for 90 min and evaporated under vacuum. ^{1}H NMR and $^{31}P\{^1H\}$ NMR spectra showed *five* sets of signals due to **1O**, *cis*-**3**, and *trans*-**3** as the minor components, and due to two major products *cis*- and *trans*-[$PtCl_2$(1-κ*P*)$_2$] (**5**) in a 2 : 1 ratio. This ratio changed to 1 : 2 (inverted) during refluxing for 18 h.

Characterisation data for *cis*-[$PtCl_2$(1-κ*P*)$_2$] (*cis*-5). ^{1}H NMR ($CDCl_3$): δ 2.15 (s, 3 H, SMe), 2.73 (t, $^3J_{HH}$ = 6.6 Hz, 2 H, SCH_2), 3.57 (q, $^3J_{HH}$ = 6.2 Hz, 2 H, HNCH_2), 4.02 (br s, 2 H, fc), 4.31 (br s, 2 H, fc), 4.41 (br s, 2 H, fc), 4.69 (br s, 2 H, fc), 6.58 (unresolved t, 1 H, NH), 7.11–7.61 (m, 10 H, PPh_2). $^{31}P\{^1H\}$ NMR ($CDCl_3$): δ 10.2 (s with ^{195}Pt satellites, $^1J_{PtP}$ = 3790 Hz).

Characterisation data for *trans*-[$PtCl_2$(1-κ*P*)$_2$] (*trans*-5). ^{1}H NMR ($CDCl_3$): δ 2.08 (s, 3 H, SMe), 2.60 (t, $^3J_{HH}$ = 6.6 Hz, 2 H, SCH_2), 3.44 (q, $^3J_{HH}$ = 6.4 Hz, 2 H, HNCH_2), 4.48 (virtual t, J = 1.8 Hz, 2 H, fc), 4.59 (virtual t, J = 1.9 Hz, 2 H, fc), 4.65 (virtual

t, J = 1.9 Hz, 2 H, fc), 4.89 (virtual t, J = 1.9 Hz, 2 H, fc), 6.37 (t, $^3J_{HH}$ = 5.9 Hz, 1 H, NH), 7.37–7.48 (m, 6 H, PPh_2), 7.61–7.70 (m, 4 H, PPh_2). $^{31}P\{^1H\}$ NMR ($CDCl_3$): δ 10.9 (s with ^{195}Pt satellites, $^1J_{PtP}$ = 2615 Hz).

Reaction of K[$PtCl_3(C_2H_4)$] with two equivalents of 1. A solution of **1** (20 mg, 0.04 mmol) in chloroform (1 mL) was added to a solution of K[$PtCl_3(C_2H_4)$] (8 mg, 0.02 mmol) in methanol (1 mL). The resulting orange-red mixture was stirred at room temperature for 90 min and evaporated. ^1H NMR and $^{31}P\{^1H\}$ NMR spectra again indicated the presence of **1O**, *cis*-**3**, and *trans*-**3** in trace amounts, and the bis(phosphine) complexes *cis*- and *trans*-**5** in the ratio of 1 : 2 as the major products. The ratio did not change during refluxing for 18 h.

X-Ray crystallography

Single-crystals suitable for X-ray diffraction analysis were grown from hexane–toluene (**1**), hexane–chloroform (*trans*-**2**·1/2H_2O, *cis*-**3**) and pentane–ethyl acetate (*trans*-**3**·1/2CH_3CO_2Et) by liquid-phase diffusion at room temperature. Crystals of **1O** were obtained similarly from hexane–ethyl acetate at −18 °C.

The diffraction data ($\pm h$ $\pm k$ $\pm l$; θ_{max} = 27.0 or 27.5°, data completeness ≥99.5%) were collected with an Apex 2 (Bruker) diffractometer equipped with Cryostream Cooler (Oxford Cryosystems) using graphite-monochromated Mo Kα radiation (λ = 0.71073 Å) and were corrected for absorption by the methods incorporated in the diffractometer software.

The structures were solved by direct methods (SHELXS97[36]) and refined by full-matrix least-squares based on F^2 (SHELXL97[36]). The non-hydrogen atoms were refined with anisotropic displacement parameters and the CH hydrogens were included at their calculated positions and refined as riding atoms. The OH and NH hydrogens were identified on the difference electron density maps and refined as riding atoms with U_{iso}(H) set to 1.2U_{eq}(O/N). Relevant crystallographic data and structure refinement parameters are summarised in Table S1 (see ESI†).

Geometric data and all structural drawings were obtained with a recent version of the PLATON program.[37] The numerical values were rounded with respect to their estimated deviations (ESDs) given to one decimal place. Parameters pertaining to atoms in constrained positions are given without ESDs.

Acknowledgements

This work was financially supported by the Czech Science Foundation (project no. 13-08890S) and is a part of the long-term research plan of the Faculty of Science, Charles University in Prague supported by the Ministry of Education, Youth and Sports of the Czech Republic (project no. MSM0021620857).

Notes and references

1 (*a*) C. A. Bessel, P. Aggarwal, A. C. Marschilok and K. J. Takeuchi, *Chem. Rev.*, 2001, **101**, 1031; (*b*) Z. Freixa and P. W. N. M. van Leeuwen, *Coord. Chem. Rev.*, 2008, **252**, 1755.

2 For selected recent examples, see: (*a*) B. P. Morgan and R. C. Smith, *J. Organomet. Chem.*, 2008, **693**, 11; (*b*) R. Schuecker, K. Mereiter, F. Spindler and W. Weissensteiner, *Adv. Synth. Catal.*, 2010, **352**, 1063; (*c*) N. Nasser, D. J. Eisler and R. J. Puddephatt, *Chem. Commun.*, 2010, **46**, 1953; (*d*) L. Kaganovsky, D. Gelman and K. Rueck-Braun, *J. Organomet. Chem.*, 2010, **695**, 260; (*e*) Y. Canac, N. Debono, C. Lepetit, C. Duhayon and R. Chauvin, *Inorg. Chem.*, 2011, **50**, 10810; (*f*) K. Ding, D. L. Miller, V. G. Young and C. C. Lu, *Inorg. Chem.*, 2011, **50**, 2545; (*g*) R. Gramage-Doria, D. Armspach, D. Matt and L. Toupet, *Chem.–Eur. J.*, 2012, **18**, 10813; (*h*) P. D. Newman, K. J. Cavell and B. M. Kariuki, *Dalton Trans.*, 2012, **41**, 12395; (*i*) C. Barthes, C. Lepetit, Y. Canac, C. Duhayon, D. Zargarian and R. Chauvin, *Inorg. Chem.*, 2013, **52**, 48; (*j*) A. G. Jarvis, P. E. Sehnal, S. E. Bajwa, A. C. Whitwood, X. Zhang, M. S. Cheung, Z. Lin and I. J. S. Fairlamb, *Chem.–Eur. J.*, 2013, **19**, 6034.

3 (*a*) N. Wang, T. M. McCormick, S.-B. Ko and S. Wang, *Eur. J. Inorg. Chem.*, 2012, 4463; (*b*) M. Jung, Y. Suzaki, T. Saito, K. Shimada and K. Osakada, *Polyhedron*, 2012, **40**, 168; (*c*) P. D. Zeits, G. P. Rachiero, F. Hampel, J. H. Reibenspies and J. A. Gladysz, *Organometallics*, 2012, **31**, 2854.

4 (*a*) J. Gil-Rubio, V. Cámara, D. Bautista and J. Vicente, *Inorg. Chem.*, 2013, **52**, 4071; (*b*) J. D. Blakemore, M. J. Chalkley, J. H. Farnaby, L. M. Guard, N. Hazari, C. D. Incarvito, E. D. Luzik and H. W. Suh, *Organometallics*, 2011, **30**, 1818; (*c*) B. P. Morgan, G. A. Galdamez, R. J. Gilliard and R. C. Smith, *Dalton Trans.*, 2009, 2020.

5 K. Tani, M. Yabuta, S. Nakamura and T. Yamagata, *J. Chem. Soc., Dalton Trans.*, 1993, 2781.

6 (*a*) I. R. Butler, M. Kalaji, L. Nehrlich, M. Hursthouse, A. I. Karaulov and K. M. A. Malik, *J. Chem. Soc., Chem. Commun.*, 1995, 459; (*b*) A. Hildebrandt, N. Wetzold, P. Ecorchard, B. Walfort, T. Rüffer and H. Lang, *Eur. J. Inorg. Chem.*, 2010, 3615.

7 The only related examples appear to be complexes containing P,S,X-terdentate ligands, in which the *trans*-position of the phosphorus and sulphur atoms results from the particular ligand geometry. For representative examples, see: (*a*) H. A. Ankersmit, N. Veldman, A. L. Spek, K. Vrieze and G. van Koten, *Inorg. Chim. Acta*, 1996, **252**, 339; (*b*) J. D. G. Correia, Â. Domingos, I. Santos and H. Spies, *J. Chem. Soc., Dalton Trans.*, 2001, 2245; (*c*) S. Bonnet, J. Li, M. A. Siegler, L. S. von Chrzanowski, A. L. Spek, G. van Koten and R. J. M. K. Gebbink, *Chem.–Eur. J.*, 2009, **15**, 3340.

8 J. Kühnert, M. Dušek, J. Demel, H. Lang and P. Štěpnička, *Dalton Trans.*, 2007, 2802.

9 P. Štěpnička, M. Krupa, M. Lamač and I. Císařová, *J. Organomet. Chem.*, 2009, **694**, 2987.

10 P. Štěpnička, B. Schneiderová, J. Schulz and I. Císařová, *Organometallics*, 2013, **32**, 5754.

11 (*a*) J. Podlaha, P. Štěpnička, J. Ludvík and I. Císařová, *Organometallics*, 1996, **15**, 543; (*b*) P. Štěpnička, *Eur. J. Inorg. Chem.*, 2005, 3787.

12 Ferrocene-based phosphine-thioether donors reported to date include phosphinoferrocenes modified with various SR and CH_2SR substituents (R = an organyl group) in positions 1′ or 2 of the ferrocene moiety. For representative examples, see: (*a*) N. J. Long, J. Martin, G. Opromolla, A. J. P. White, D. J. Williams and P. Zanello, *J. Chem. Soc., Dalton Trans.*, 1999, 1981; (*b*) J. E. Aguado, S. Canales, M. C. Gimeno, P. G. Jones, A. Laguna and M. D. Villacampa, *Dalton Trans.*, 2005, 3005; (*c*) V. C. Gibson, N. J. Long, A. J. P. White, C. K. Williams, D. J. Williams, M. Fontani and P. Zanello, *J. Chem. Soc., Dalton Trans.*, 2002, 3280; (*d*) L. Routaboul, S. Vincendeau, J.-C. Daran and E. Manoury, *Tetrahedron: Asymmetry*, 2005, **16**, 2685; (*e*) R. Malacea, L. Routaboul, E. Manoury, J.-C. Daran and R. Poli, *J. Organomet. Chem.*, 2008, **693**, 1469; (*f*) E. M. Kozinets, O. Koniev, O. A. Filippov, J.-C. Daran, R. Poli, E. S. Shubina, N. V. Belkova and E. Manoury, *Dalton Trans.*, 2012, **41**, 11849; (*g*) J. Priego, O. G. Mancheño, S. Cabrera, R. G. Arrayás, T. Llamas and J. C. Carretero, *Chem. Commun.*, 2002, 2512; (*h*) O. G. Mancheño, J. Priego, S. Cabrera, R. G. Arrayás, T. Llamas and J. C. Carretero, *J. Org. Chem.*, 2003, **68**, 3679; (*i*) O. G. Mancheño, R. G. Arrayás and J. C. Carretero, *Organometallics*, 2005, **24**, 557; (*j*) S. Cabrera, R. G. Arrayás and J. C. Carretero, *Angew. Chem., Int. Ed.*, 2004, **43**, 3944.

13 P. Štěpnička, *Chem. Soc. Rev.*, 2012, **41**, 4273.

14 (*a*) A. El-Faham and F. Albericio, *Chem. Rev.*, 2011, **111**, 6557; (*b*) E. Valeur and M. Bradley, *Chem. Soc. Rev.*, 2009, **38**, 606.

15 R. G. Pearson, *J. Am. Chem. Soc.*, 1963, **85**, 3533.

16 (*a*) F. R. Hartley, *The Chemistry of Platinum and Palladium*, Applied Science, London, 1973; (*b*) L. Sacconi, F. Mani and A. Bencini, in *Comprehesive Coordination Chemistry*, ed. G. Wilkinson, R. D. Gillard and J. A. McCleverty, Pergamon Press, Oxford, 1987, vol. 5, ch. 5, p. 1; (*c*) C. F. J. Barnard and M. J. H. Russell, in *Comprehesive Coordination Chemistry*, ed. G. Wilkinson, R. D. Gillard and J. A. McCleverty, Pergamon Press, Oxford, 1987, vol. 5, ch. 51, p. 1099; (*d*) A. T. H. Hutton and C. P. Morley, in *Comprehesive Coordination Chemistry*, ed. G. Wilkinson, R. D. Gillard and J. A. McCleverty, Pergamon Press, Oxford, 1987, vol. 5, ch. 51.9, p. 1157; (*e*) D. M. Roundhill, in *Comprehesive Coordination Chemistry*, ed. G. Wilkinson, R. D. Gillard and J. A. McCleverty, Pergamon Press, Oxford, 1987, vol. 5, ch. 52, p. 351.

17 Some of the signals become well resolved at 50 °C.

18 Reaction performed under milder conditions (room temperature/1 h) afforded a mixture containing *cis*-**3** and *trans*-**3** in an approximate 75 : 25 ratio, which apparently reflects kinetic inertness of Pt(II) and the geometry of the leaving ligand. Also seen was a signal attributable to *cis*-**5** at δ_P 10.15 with $^1J_{PtP} \approx 3800$ Hz, which was not detected in the reaction mixture obtained after refluxing for 3 h.

19 In analogy to bis-phosphine complexes of the type $[PtCl_2L_2]$, the $^1J(^{195}Pt,^{31}P)$ coupling constants in *cis* isomers can be expected to be larger than in *trans* isomers: (*a*) Ref. 16*a*, ch. 7, pp. 138–140 (*b*) P. S. Pregosin and R. W. Kunz, in *NMR Basic Principles and Progress*, ed. P. Diehl, E. Fluck and R. Kosfeld, Springer, Berlin, 1979, vol. 16, ch. E, p. 65.

20 (*a*) T. G. Appleton, H. C. Clark and L. E. Manzer, *Coord. Chem. Rev.*, 1973, **10**, 335; (*b*) Ref. 16*a*, ch. 11, p. 299 ff.

21 A. G. Orpen, L. Brammer, F. H. Allen, O. Kennard, D. G. Watson and R. Taylor, *J. Chem. Soc., Dalton Trans., Suppl.*, 1989, S1.

22 R. G. Pearson, *Inorg. Chem.*, 1973, **12**, 712.

23 Complexes of the type $[PtCl_2(PR_3)(SR_2)]$ (without chelating P,S-donors), whose crystal structure is known, adopt *cis*-configuration: (*a*) H.-P. Abicht, K. Jurkschat, K. Peters, E.-M. Peters and H. G. von Schnering, *J. Organomet. Chem.*, 1989, **364**, 415; (*b*) M. N. I. Khan, C. King, J. P. Fackler Jr. and R. E. P. Winpenny, *Inorg. Chem.*, 1993, **32**, 2502; (*c*) I. Michaud-Soret, J. Kozelka and C. Bois, *Acta Crystallogr., Sect. C: Cryst. Struct. Commun.*, 1993, **49**, 589; (*d*) P. Kapoor, K. Lövqvist and Å. Oskarsson, *J. Mol. Struct.*, 1998, **470**, 39.

24 Steric strain resulting from *trans*-chelate coordination can be expected to operate in accord with *trans*-influence in this case.

25 Compare, for instance, the covalent radii being 1.39 Å for Pd, and 1.36 Å for Pt. This similarity is attributed to lanthanide contraction affecting the heaviest Group 10 metal. The radii are quoted from: B. Cordero, V. Gómez, A. E. Platero-Prats, M. Revés, J. Echeverría, E. Cremades, F. Barragán and S. Alvarez, *Dalton Trans.*, 2008, 2832.

26 The orientation of the C24–C25 bond is nearly the same in all three *complexes*. Compare the angles subtended by the vector of the C24–C25 bond and the Cp1 plane being 33.0(1)° in **1**, 54.7(1)° in *trans*-**2**, 55.4(2)° in *trans*-**3**, and 56.3(2)° in *cis*-**3**.

27 E_{pa} and E_{pc} are anodic and cathodic peak potentials, respectively. Potentials determined at the scan rate 0.1 V s^{-1} are quoted for all irreversible processes.

28 The anodic peak current (i_{pa}) was directly proportional to the square root of the scan rate ($i_{pa} \propto \nu^{1/2}$), which suggests the oxidation to be a standard diffusion-controlled redox transition.

29 Chemical reactions following an electron transfer process are well documented for phosphinoferrocenes. For examples, see: (*a*) J. H. L. Ong, C. Nataro, J. A. Golen and A. L. Rheingold, *Organometallics*, 2003, **22**, 5027; (*b*) P. Zanello, G. Opromolla, G. Giorgi, G. Sasso and A. Togni, *J. Organomet. Chem.*, 1996, **506**, 61; (*c*) G. Pilloni, B. Longato and B. Corain, *J. Organomet. Chem.*, 1991, **420**, 57. See also ref. 11*a*.

30 Ferrocene itself showed practically identical response under the experiment conditions. The observed peak separations are higher than the theoretically predicted values

(59 mV at 25 °C), presumably due to a high resistance of the analysed solution. No *iR* drop correction was applied to the data.

31 C. Hansch, A. Leo and R. W. Taft, *Chem. Rev.*, 1991, **91**, 165.

32 The process is controlled by diffusion ($i_p \propto \nu^{1/2}$); the separation of the peaks in cyclic voltammogram is 80 mV at a scan rate of 0.1 V s^{-1}.

33 C. Amatore and A. Jutand, *Acc. Chem. Res.*, 2000, **33**, 314 and references cited therein.

34 D. Drew and J. R. Doyle, *Inorg. Synth.*, 1972, **13**, 47.

35 P. B. Chock, J. Halpern and F. E. Paulik, *Inorg. Synth.*, 1990, **28**, 349.

36 G. M. Sheldrick, *Acta Crystallogr., Sect. A: Fundam. Crystallogr.*, 2008, **64**, 112.

37 A. L. Spek, *J. Appl. Crystallogr.*, 2003, **36**, 7.